AAC Accepted Manuscript Posted Online 16 November 2015
Antimicrob. Agents Chemother. doi:10.1128/AAC.02203-15

Identification of a pyridoxine-derived small-molecule inhibitor targeting dengue virus RNA-dependent RNA polymerase

Hong-Tao Xu,[a] Susan P. Colby-Germinario,[a] Said Hassounah,[a] Peter K. Quashie,[a] Yingshan Han,[a] Maureen Oliveira,[a] Brent R. Stranix,[b] and Mark A. Wainberg[a,c,d*]

[a]McGill University AIDS Centre, Lady Davis Institute for Medical Research, Jewish General Hospital, Montreal, Quebec, Canada and Departments of [c]Medicine and [d]Microbiology and Immunology, McGill University, Montreal, Quebec, Canada. [b]Champlain Exploration Pharma Inc., Montreal, Quebec, Canada.

Running title: Dengue virus RNA-dependent RNA polymerase inhibitor

* To whom correspondence should be addressed: Mark A. Wainberg, Ph.D., McGill University AIDS Centre, Lady Davis Institute for Medical Research, Jewish General Hospital, 3755 Côte-Ste-Catherine Rd, Montreal, Quebec, H3T 1E2, Canada Tel: (514) 340-8260; Fax: (514) 340-7537; E-mail: mark.wainberg@mcgill.ca

Word count:

Abstract: 250 words

Text: 5526 words

Tables: 6

Figures: 5

Acknowledgments

This work was partly supported by research grants from the Canadian Institutes of Health Research (CIHR). Mark A. Wainberg is a consultant to Champlain Biosciences Inc.

ABSTRACT

The viral RNA-dependent RNA polymerase (RdRp) activity of the dengue virus (DENV) NS5 protein is attractive target for drug design. Here, we report the identification of a novel class of inhibitor, i.e. an active-site metal-ion chelator, that acts against DENV RdRp activity. DENV RdRp utilizes two-metal ion mechanism of catalysis; therefore, we constructed a small library of compounds, through mechanism-based drug design, aimed at chelating divalent metal ions in the catalytic site of DENV RdRp. We now describe a pyridoxine-derived small-molecule inhibitor that targets DENV RdRp and show that 5-benzenesulfonylmethyl-3-hydroxy-4-hydroxymethyl-pyridine-2-carboxylic acid hydroxyamide (termed DMB220) inhibited the RdRp activity of DENV sereoytypes 1-4 at low µM 50% inhibitory concentrations (IC_{50s} of 5-6.7 µM) in an enzymatic assay. The antiviral activity of DMB220 against DENV infection was also verified in cell-based assay and showed a 50% effective concentration (EC_{50}) <3 µM. Enzyme assays proved

that DMB220 was competitive with nucleotide incorporation. DMB220 did not inhibit the enzymatic activity of recombinant HIV-1 reverse transcriptase and showed only weak inhibition of HIV-1 integrase strand-transfer activity, indicating high specificity for DENV RdRp. S600T substitution in the DENV RdRp, that was previously shown to confer resistance to nucleoside analogue inhibitors (NI) conferred 3-fold hyper-susceptibility to DMB220 and enzymatic analyses showed that this hyper-susceptibility may arise from the decreased binding/incorporation efficiency of the natural NTP substrate without significantly impacting on inhibitor binding. Thus, metal ion chelation at the active site of DENV RdRp represents a viable anti-DENV strategy and DMB220 is a first of class DENV inhibitor.

Keywords

Dengue virus, antiviral, RNA-dependent RNA polymerase, non-nucleoside inhibitor, metal-chelating inhibitor

INTRODUCTION

Dengue virus (DENV) belongs to the family *Flaviviridae*, a group of enveloped positive-sense single-stranded RNA viruses that includes the genera *Hepacivirus* (prototype, hepatitis C virus), *Flavivirus* (prototype, yellow fever virus), and *Pestivirus* (prototype, bovine virus diarrhoea) (1). Distinct from the hepaciviruses and pestiviruses which are not arthropod-borne, the flaviviruses are transmitted by mosquitos and ticks. Dengue, the most prevalent arthropod-borne viral disease of humans, is caused by four serotypes (DENV 1-4) and has had major impact on global public health (2-4).

Infection with any of the DENV serotypes may result in a wide spectrum of clinical symptoms ranging from a mild flu-like syndrome (known as dengue fever [DF]) to the most severe forms of the disease, which are characterized by coagulopathy, increased vascular fragility, and permeability (dengue hemorrhagic fever [DHF]). The latter may progress to hypovolemic shock (dengue shock syndrome [DSS])(3, 5). Among the four serotypes, DENV-2 is the most prevalent on a global scale, followed by DENV-3, DENV-1 and DENV-4(6). Dengue is endemic in over 100 tropical and sub-tropical countries and the global incidence of dengue has grown dramatically in recent decades(7).

Half of the world's population is now at risk of dengue infection and ~400 million people experience DENV infections annually (8), with 500,000 cases of DHF/DSS and 22,000 deaths (http://www.who.int/csr/disease/dengue/impact/en/, accessed July 6, 2015).There is currently no specific antiviral treatment or preventive vaccine for dengue. Despite

decades of efforts, developing a preventive dengue vaccine remains challenging because a vaccine must provide long-lasting protection against all four DENV serotypes (tetravalent dengue vaccine) and not be prone to potential side effects of non-neutralizing, serotype-cross-reactive immune responses (9-11).

Secondary heterotypic DENV infection is associated with an increased risk of severe disease as a result of an immune-pathological component in dengue pathogenesis, which is referred to as antibody-dependent enhancement. Although progress in vaccine development has been made, there is an obvious need to also develop anti-DENV antivirals (for reviews see (12-21)).

The DENV NS5 protein is an important target of DENV drug discovery efforts (15).NS5 is about 900 amino acids long and comprises a methyl transferase domain at its N terminus and an RNA-dependent RNA polymerase (RdRp) domain at the C terminus. NS5 is the most conserved of DENV viral proteins and the crystal structures of NS5 and its polymerase domain have been solved (22-24). The DENV RdRp possesses a half-closed right hand architecture, which is conserved among different classes of DNA and RNA polymerases (24). Within the subdomains termed finger, palm and thumb, 6 conserved motifs, termed A-F, play key roles in RNA, NTP, and metal-ion binding and catalysis (24). The amino acids in the catalytic site of DENV RdRp are located within motifs A (aspartate at position 533, D533) and a catalytic triad GDD at position 662–664 in motif C. These aspartate residues are involved in the coordination of two divalent Mg++ cofactors that are essential to the catalytic process, i.e. the “two-metal-ion

mechanism" (25).The DENV RdRp, like those of other members of the *Flaviviridae* family, carries out viral RNA synthesis through a *de novo* initiation mechanism(26). Moreover, RdRp activity is essential for viral replication. Since there is no mammalian host cellular enzyme equivalent, no issues of toxicity should be anticipated if specific inhibitors of DENV RdRp activity can be developed (15, 19).

Investigational DENV RdRp inhibitors can be grouped into two classes, nucleoside analogue inhibitors (NIs) and non-nucleoside analogue inhibitors (NNIs), (for reviews see (15, 16, 19, 21)). NIs require intracellular phosphorylation to a 5'-triphosphate form by cellular kinases; they then bind at the enzyme active site and compete with natural substrates for incorporation and this is followed by chain termination (27, 28). NNIs do not require intracellular activation and provide an alternative mechanism by binding to allosteric sites remote from the active site of the RdRp and interfere with the chemical step of RNA synthesis (15, 16, 19). No NIs or NNIs have been approved for clinical treatment of DENV infections.

Metal chelating agents represent an important class of viral enzyme inhibitors (29-33). Chelation of the divalent Mg++ cofactors of HIV integrase has proven to be a successful strategy in the design of HIV integrase inhibitors and resulted in approval of the chelating inhibitors raltegravir (RAL), elvitegravir (EVG) and dolutagravir (DTG) (for review, see (31)). Metal chelation was also effective at inhibiting HCV polymerase (34, 35) and the influenza PA endonuclease activity (33). *A similar concept for the development of*

compounds bearing chelating motifs that are able to bind the bivalent metal ions in the catalytic site of DENV RdRp has not previously been tested.

In this study, we report on a novel inhibitor of DENV RdRp, i.e. 5-benzenesulfonylmethyl-3-hydroxy-4-hydroxymethyl-pyridine-2-carboxylic acid hydroxyamide (termed DMB220). The pyridoxine-derived small-molecule inhibitor DMB220 was identified through the screening of a small library of small molecule compounds, constructed through mechanism-based drug design aimed at chelating divalent metal ions at the catalytic sites of such viral enzymes as HIV integrase and viral RNA-dependent RNA polymerase (36). DMB220 has a broad spectrum of inhibitory activity against the RdRp enzymes all of four DENV serotypes. The inhibitory activity of DMB220 can be reversed by enhancing concentrations of the natural ribonucleotide substrate. Furthermore, we show that the DENV RdRp variant S600T, which was shown to be resistant to nucleoside analogue inhibitors (27), is hyper-susceptible to DMB220. Thus, metal ion chelation is a potential approach in anti-DENV antiviral development and DMB220 may be a first of class potent pan-serotypic RdRp inhibitor for DENV replication.

Materials and Methods

Reagents and nucleic acids

The (-)3'UTR RNA, which contains the last 380 nucleotides (nt) of the negative strand of DENV2 genome plus 3 extra guanines upstream of its 5' terminus, was synthesized using an Ambion T7-MEGAscript kit (Invitrogen, Burlington, ON, Canada) as described

(27). T7 transcription was performed on PCR product amplified from plasmid pBAC-DENV-FL DNA which contains the full length cDNA of the DENV NGC strain (37) (kindly provided by Drs. Jose A. Usme-Ciro and Juan C. Gallego-Gomez, Universidad de Antioquia, Colombia). RNA was purified by 8% polyacrylamide-urea gel electrophoresis. 3'dGTP was obtained from TriLink BioTechnologies (San Diego, CA). Mycophenolic acid (MPA) was obtained from Sigma-Aldrich (Markham, ON, Canada). The plasmid pET21a[His-Strep-DENV2_NS5 DNA] (38) was kindly provided by Dr. Matthias Götte, University of Alberta, Canada.

Preparation of DMB-220

DMB220 was identified through screening a small library of small molecule compounds (36) constructed through mechanism-based drug design aimed at chelating the divalent metal ions within the catalytic site of viral enzymes such as HIV integrase and viral RNA-dependent RNA polymerase. For chemical preparation of DMB220 (Fig. 1.), 550 mg isopropylidene pyridoxine dissolved in 30 mL DCM was reacted with 2.5 equivalents of methane sulfonyl chloride in the presence of 5 equivalents triethyl amine. Extraction with 5% citric acid, drying over Na_2SO_4, and evaporation yielded 500mg of desired mesylate. This was immediately reacted with 400 mg of benzene sulfinic acid in 2 mL DMF. The product was isolated by precipitation in water and filtration to give a 85% yield. The crude was dissolved in $CHCl_3$30mL and 400 mg mCPBA was added. After 1 h stirring, the reaction was extracted using K_2CO_3 and the organic phase dried over $CaCO_3$ and the evaporated. The residue was dissolved in 3 mL DCM and 3mL trifluoroactetic anhydride (TFAA) was added. Stirring at reflux 45^{o}C for 20 h affording

the rearranged product, isolated through quantitative evaporation of solvent. The residue was then added to a solution of MnO_2 2g in $CHCl_3$ (30 ml) and stirred at reflux 1h. Filtration and evaporation yielded the aldehyde (250 mg). This was placed in 10 mL MeOH with 1.2 eq I_2 and 3 eq KOTMS. Stirring at room temperature for 1h yielded the ester via quantitative conversion. The product was purified on silica gel. Then 100 mg of the ester was reacted with excess (hydroxylamine 50% aq) in pyridine to give the hydroxamate. Dilution in EtOAc and extraction via 5% citric acid gave the desired intermediate. The final product was obtained by adding 50 mg of the above acetonide to neat 70% formic acid. After 15 min the reaction was complete, the formic acid was evaporated off and the residue triturated with water to yield DMB220as a white powder (41% yield). Stock solution at 10 mM was prepared by dissolving DMB220 in 100% DMSO. Storage was in small aliquots at -80^{o}C.

Purification of His_6-tagged recombinant DENVNS5 polymerase domains

The expression vectors used in this study are all T7 promoter-driven. Plasmid pET21a[His-Strep-DENV2_NS5 DNA] containing the NS5 polymerase domain of DENV2 NGC strain (38) was transformed into Novagen Rosetta 2 (DE3) competent cells (EMD Millipore, Etobicoke, ON, Canada)and used for purification of the NS5 RNA-dependent RNA polymerase (RdRp) domain with a N-terminal His_6 tag of the DENV2 NGC strain, based on previously described protocols with minor modifications (38, 39). For construction of an S600T mutant DENV2 NS5 polymerase, we performed site-directed mutagenesis using the Stratagene Quick Change II XL site-directed mutagenesis

kit on pET21a[His-Strep-DENV2_NS5 DNA]. DNA sequencing of the complete RdRp domain was performed to verify the absence of spurious substitutions .

For purification of the RdRp domains of the other three serotypes DENV1 (US/Hawaii/1944), 3 (MY00-22366) and 4 (MY01-22713), cDNAs encoding the RdRp domains of DENV1, 3 and 4 (23) were cloned into a pNIC-Bsa4 vector bearing a TEV cleavage site downstream of the N-terminal His_6 tag (kindly provided by Dr. Julien Lescar, Nanyang Technological University, Singapore); the plasmid DNAs pNIC-Bsa4[DENV1_NS5], pNIC-Bsa4[DENV3_NS5] and pNIC-Bsa4[DENV4_NS5] were transformed into Rosetta 2 (DE3) competent cells (EMD Millipore-Novagen, Etobicoke, ON, Canada).The bacterial cells were cultured in LB medium supplemented with carbenicillin (100 µg/ml) for the pET21a construct or kanamycin (50 µg/ml)for the pNIC-Bsa4 construct at 37^{o}C until the optical density at 600 nM reached 0.6-0.8. After induction of expression with 0.4 mM isopropyl β-D-1-thiogalactopyranoside (IPTG) in the presence of 50 µM $MgCL_2$ and 50 µM $ZnCL_2$, the cells were grown for 18 hours at 15 ^{o}C with a shaking speed of 250 rpm. Cells were harvested by centrifugation, re-suspended in lysis buffer containing 20 mM Tris-HCL pH7.5, 5% glycerol, 10 mM imidazole, 300 mM NaCL, 0.1% Igepal-CA630, 10 U/ml Benzonase, and 1 x complete EDTA-free protease inhibitors cocktail (Roche, Mississauga, ON, Canada). Cells were lysed by sonication, and the extract was cleared by centrifugation at 18,500 x g for 30 min at 4 ^{o}C. The clarified supernatant was loaded onto a Ni-nitrilotriacetic acid (Ni-NTA) column (Novagen) equilibrated with lysis buffer. The Ni-NTA column was washed and eluted with lysis buffer containing a gradient of imidazole from 20 mM to 500 mM.

Fractions containing polymerase were combined and dialyzed overnight against dialysis buffer (10 mM Tris-HCL, pH 7.5, 300 mM NaCL, 20% glycerol, 5 mM $MgCL_2$). After dialysis, proteins were diluted with an equal volume of dialysis buffer without NaCl and bound to Heparin Sepharose 6 Fast Flow (GE Healthcare). The bound proteins were then eluted with a gradient of NaCl (0–0.6M) in dialysis buffer. Protein concentrations were measured by a Bradford protein assay kit (Bio-Rad Laboratories, Saint-Laurent, QC, Canada). After final dialysis, the purified DENV NS5 polymerase domains were stored at −80°C .

In vitro filter-binding DENV RdRp assay

The filter-binding DENV RdRp assay was adapted from a published protocol(27) with modifications. Briefly, the reaction samples consisted of 40 nM enzyme, 10 nM (-) 3'UTR RNA, mixed together in RdRp assay buffer containing 40 mM Tris-HCL, pH 7.0, 10 mM NaCL, 2 mM $MgCl_2$, 0.001% Triton X-100, and 10 µM cysteine. Reactions were initiated at 30°C by adding 200µM each of ATP, GTP, UTP and 0.9 µM ^{3}H-CTP in a final volume of 20 µL. The reactions were allowed to proceed up to 180 min and were terminated by adding 0.2 mL of 10% cold trichloracetic acid (TCA) and 20 mM sodium pyrophosphate containing 5µg herring sperm DNA carrier and incubated for at least 30 min on ice. The precipitated products were filtered onto a 96-well MutiScreen HTS FC filter plate (Millipore, Etobicoke, ON). The filter plate was pre-wet with 150 µL assay buffer prior to use and sequentially washed with 200 µL of 10% TCA and 150 µL of 95% ethanol. The radioactivity of incorporated products was analyzed by a 1450 MicroBeta

TriLux Microplate Scintillation and Luminescence Counter (Perkin Elmer, Waltham, MA).

Steady-state kinetic analysis

Measurements of steady-state kinetic parameters were performed as described (27). To determine the Michaelis-Menten constants (Km) and Vmax for the NTP substrate in the filter-binding DENV RdRp assay, NTPs were serially diluted to provide a range of substrate concentrations. The NTPs (containing ^{3}H -CTP as tracer) concentrations tested ranged from 0.02 µM to 50 µM at 3-fold serial dilutions, and the RNA concentration was fixed at 200 nM. All data were analyzed using GraphPad Prism5.0 software (GraphPad Software, San Diego, CA) according to the instructions of the software provider.

Inhibitory effects of DMB220 on DENV RdRp activity

Measurement of the inhibitory effect of compounds on DENV NS5RdRp activity was accomplished by evaluating the amount of radiolabeled CTP incorporated by the enzyme into newly synthesized RNA using the filter-binding RdRp assay and a DENV (-)3'UTR RNA template essentially as described (27). The final assay reaction mixtures contained multiple concentrations of serially diluted test compounds,40 nM enzyme, and 10 nM (-) 3'UTR RNA in assay buffer containing 40 mM Tris-HCL, pH 7.0, 10 mM NaCL, 1 mM $MgCl_2$ and 0.5 mM $MnCL_2$, 0.001% Triton X-100, and 10 µM cysteine. Reactions were started at 30^{o}C by adding NTP substrate containing ^{3}H-CTP as tracer in a final volume of 20 µL. The reactions were terminated and processed as described above for the RdRp assay. The IC50 values were determined by nonlinear regression using

GraphPad Prism5.0 software (GraphPad Software, San Diego, CA) according to instructions of the software provider.

Evaluation of inhibitory efficiencies of compounds against dengue virus replication in cell culture

The viruses DENV1 (Hawaii, TVP 17788), DENV2 NGC strain, DENV3 (H87, TVP 15322), and DENV4 (TVP 13886) (kindly provided by Dr. Robert B. Tesh, University of Texas Medical Branch) and BHK-21 cells (Baby hamster kidney cells; ATCC CCL10) were used in the cell-based antiviral assays. The viral stock was prepared by inoculation of C6/36 cells (*Aedes albopictus* clone C6/36cells; ATCC CRL166) as described (40). Infected cells were maintained in RPMI-1640 (Invitrogen, Burlington, ON, Canada) medium containing 2% fetal bovine serum (FBS) and 0.5% penicillin/streptomycin stock at 28^{o}C in a 5% CO2 incubator for 7 days until the cells showed cytopathic effects (CPE). The supernatant was cleared by centrifugation at 2,000 x g for 5 min to remove cell debris and adjusted to 20 % FBS. Aliquots of virus were stored at -80^{o}C. The 50% tissue culture infective dose ($TCID_{50}$) was determined by the Promega Viral ToxGlo Assay (Fisher Scientific, Ottawa, ON, Canada) using BHK-21 cells as instructed by the manufacturer. Cell-based assays for evaluation of antiviral activity against DENV were essentially performed as described (41, 42) with modifications using the Viral ToxGlo Assay (Fisher Scientific, Ottawa, ON) as instructed by the manufacturer. Briefly, BHK-21 cells were plated into 96 well plates at 2,500 cells/well in DMEM containing 10% FBS and 1% penicillin/streptomycin. Cells were incubated at 37°C overnight and infected with 100 $TCID_{50}$ of DENV for 90 min. The media were then replaced by DMEM

containing 2.5 % FBS with variable concentrations of test compounds. Cell cultures were maintained at 37°C in a 5% CO2 incubator for 3 days. The Viral Tox reagent was prepared fresh and 100µl reagent were added to each well. Plates were incubated for at least 10 minutes and then quantitated by a 1450 MicroBeta TriLux Microplate Scintillation and Luminescence Counter (Perkin Elmer, Waltham, MA). For an off-target cytotoxicity assay, test compounds were processed in the same way as described above except without DENV infection of the cells. The luminescence readings were plotted against the log transformation of the concentration of the compound. Data were analyzed by nonlinear regression using GraphPad Prism5.0software (GraphPad Software, San Diego, CA).

DMB-220 inhibition of HIV-1 RT activity

Subtype B HIV-1 wild-type RT and that containing the M184V substitution were generated as described previously(43, 44).A test of the inhibitory effect of DMB-220 on HIV-1 RT activity was performed as described (45).The reaction mixture (50 µl) contained 50 mM Tris-HCL (pH 7.8), 5 mM $MgC1_2$, 2 mM ATP, 60 mM KCL, 5 mM DTT, 1 µM [^{3}H]-dTTP, 5 µg/ml of template/primer poly (rA)/(oligo(dT)$_{12-18}$(Midland Certified Reagent Company, Midland, TX), recombinant RTs of the same activity, and variable amounts of DMB-220. After incubation for30 min at 37 ^{o}C. The reactions were terminated and processed as described above for the RdRp assay.

DMB-220 inhibition of HIV-1 integrase strand transfer activity

Recombinant subtype B HIV-1 integrase was expressed in the BL21 (DE3) bacterial strain and purified as published (46, 47). The susceptibility of HIV recombinant integrase to DMB220 and integrase strand transfer inhibitors (INSTIs) was assessed by strand transfer assay (46, 47) in the presence of DMB220 or INSTIs including DTG, EVG and RAL. Compounds were diluted in compound assay buffer (50 mM MOPS, pH 6.8, 50 µg/mL BSA, 0.15% CHAPS, 50 mM NaCl, and 30 mM $MnCl_2$) plus 10% DMSO to concentrations between 0-1000 nM for INSTIs and 0-100 µM for DMB220. DNA-BIND 96-well plates (Corning) were coated with pre-processed LTR DNA blocked and washed before the addition of purified recombinant proteins. Purified HIV integrase protein in assay buffer supplemented with 5 mM DTT was added to each well and incubated for 30 min at room temperature. 25 µL of diluted INSTIs or DMB220 were added to each well followed by 25 µL of appropriately diluted biotinylated target DNA duplex. This was followed by a 1 h incubation at 37°C. Integrated target DNA was detected after washes through the use of europium-labeled streptavidin molecules as described (46, 47). The 50% inhibitory concentrations (IC_{50}s) of test compounds were determined by nonlinear regression analysis using GraphPad Prism5.0 software (GraphPad Software, San Diego, CA).

Molecular modeling

The Dengue polymerase structure PDB ID:2J7U was prepared as an Autodock receptor using autodock tools. Docking of the compound was performed using methods similar to those of previous publications (27), (48). The possible location of a putative second active site Mg++ ion was superimposed into the 2J7U structure of the HIV RT structure

1RTD by partial active site overlays. The minimal region for active site overlays was obtained by multiple partial sequence alignments between the dengue polymerase and HIV RT polymerase active sites using T-COFFEE (49). Prior to compound docking, a short single RNA strand (5'UUUAGUU) was retrieved from the PDB structure 1WMQ (50) and docked into the prepared 2J7U structure. All twenty docked poses showed that the RNA inserted into the RNA binding groove.

Subsequent compound docking was performed on the top two conformations. The 3-dimensional structure of the inhibitory compound (5-Benzenesulfonylmethyl-3-hydroxy-4-hydroxymethyl-pyridine-2-carboxylic acid hydroxyamide) was modeled and optimized for pH7.0 using the program ChemBioDrawUltra 12.0 (www.cambridgesoft.com). The compound was then docked into the active site residue of dengue polymerase, into a grid box centered on the D533 and D663 residues, with grid box dimensions (x,y,z) of 30Å, 30Å, 30Å. All ligands and receptors were prepared using Autodock Tools V1.5.6 and docked using Autodock Vina. Image processing was performed using PyMol.

Results

Purification and characterization of recombinant NS5 polymerase from DENV1, 2, 3, and 4

Recombinant NS5 polymerase domains from DENV1, 2, 3 and 4 were purified to >95% homogeneity as demonstrated by SDS-PAGE (Fig.2A). For characterization of enzyme activity, the rate of RNA synthesis was analyzed by following the incorporation of radiolabelled nucleotide into the newly synthesized RNA, which was separated from free radiolabeled nucleotide by TCA precipitation and filtration. Time course experiments

were initiated by mixing together 40 nM purified NS5 polymerase from each of the four DENV serotypes with 10 nM RNA in RdRp assay buffer; this permitted a comparison of the rates of nucleotide polymerization by NS5 polymerase for all four serotypes(Fig. 2B). We observed that the NS5 polymerase of DENV4 was the most active among the four enzymes with polymerization rates following the order: DENV4>DENV2>DENV3≥DENV1(Fig. 2B). This result is somewhat different from those of previous reports (27), which showed that the ranking order was DENV2>DENV3>DENV4>DENV1, a discrepancy that may arise from differences in the NS5 polymerase sequences used in the two studies. Steady-state kinetic analyses showed that the Km values for NTPs of NS5 polymerase of all four serotypes ranged from 3.3 - 4.0 μM (Table 1). The catalytic efficiency (K_{cat}/K_m) of the polymerase of the four serotypes followed the same ranking order as observed in the time course RdRp assay (Fig. 2B).

Inhibitory effects of DMB220 on DENV RdRp activity.

We used an in vitro filter-binding DENV RdRp assay to determine the inhibitory effects of DMB220 on DENV NS5 polymerase activity. We showed that DMB220 was potent against NS5 polymerase activity of all four serotypes (Fig. 3.) with IC50s ranging between 5.0-6.7 μM (Table 2).We also observed a 3-fold decrease in IC50 for the S600T mutated RdRp, suggesting that this variant was hyper-susceptible to DMB220. The S600T mutant was chosen for this study based on the fact that this residue is highly conserved in the RdRp **B** motif and was previously shown to be resistant to nucleoside analogue inhibitors(27). As an internal control for the filter-binding RdRp assay, we

measured the inhibitory effect of a nucleoside chain terminator 3'dGTP on DENV1-4 NS5 polymerase. We showed that 3'dGTP inhibited RdRp activity with similar potency with IC50s obtained ranging between 0.4-0.6 μM, in agreement with previous reports on the inhibitory potency of 3'dGTP on DENV NS5 polymerase activity (51). The S600T mutant enzyme did not show resistance to 3'dGTP (Table 2).

Antiviral activity of DMB220 against DENV in a cell-based assay

To validate the anti-DENV activity of DMB220 in cell culture, we used the Promega Viral ToxGlo Assay and BHK-21 cells. DENV-infected cells were treated with increasing concentrations of DMB220 and protection from cytopathic effect was measured. We used mycophenolic acid (MPA) as a positive control of inhibition of viral replication. The data show that DMB220 was able to inhibit all four serotypes of DENV with EC50s ranging between 2.2-2.8 μM (Table 3),whereas the anti-DENV potency of MPA ranged between 0.4 to 0.6 μM across the four serotypes, in agreement with previous reports (52, 53).The CC50 of DMB220 was 18 μM as assayed in BHK-21 cells using the Viral ToxGlo Assay (Table 3). *Thus, the selectivity index (SI) values of DMB220 were 6.4-8.2 as determined by the ratio of CC50 to EC50, which were lower than those of the reference compound MPA (SI: 83-125). Accordingly, DMB220 is potentially more toxic than MPA.*

Effect of NTP concentration on inhibitory potency of DMB220 against DENV polymerase activity

DMB220 was designed to be able to chelate divalent metal ions at the active site of the DENV RdRp, therefore, its binding to the RdRp active site might be competitive with that of natural NTP substrates. To assess this in reactions that were initiated by adding 3'(-)UTP RNA template at 30 ^{o}C over 120 min, we varied NTP concentrations. We found that the IC50 of DMP220 increased as higher concentrations of the nucleotide substrate were used, which suggests a competitive mechanism of action for DMB220 (Table 4). We also tested the inhibitory potency of DMB220 at various concentrations of the RNA substrate. In this circumstance, we did not observe variations in IC50s (data not shown).

Mechanism of mutated S600T RdRp hyper-susceptibility to DMB220

The S600T substitution resulted in 3-fold hyper-susceptibility to DMB220. This hyper-susceptibility may arise from facilitation of inhibitor binding and/or from diminished binding/incorporation of the natural NTP substrate. To determine the underlining mechanism of DMB220 hyper-susceptibility associated with S600T substitution, we compared the enzyme kinetic parameters of the DENV2 NS5 WT and S600T enzymes (Table 5). We measured the steady-state kinetic constant Km for the natural nucleoside substrate NTP and the inhibition constant Ki for DMB220 using (-)3'UTR RNA as template. Determinations of Ki were performed by the Dixon Plot method (Fig. 4.). Ratios of Ki/Km were calculated to determine the ability of each enzyme to selectively bind DMB220 relative to the natural nucleotide substrate. The steady state Km value of the S600T enzyme was shown to be 3-fold that of the WT, suggesting that the S600T mutant enzyme binds/incorporates the natural nucleotide substrate with decreased

efficiency compared to that of WT RT. However, the Ki value of the S600T enzyme for DMB220 was similar to that of the WT counterpart. The S600T enzyme showed decreases in Ki/Km of 0.3-fold compared with WT enzyme for DMB220, suggesting increased binding of this inhibitor. These results further support the notion that DMB220 competes with NTP at the active site of the RdRp. Our work also showed that the S600T mutant enzyme shows a 7-1-fold drop in catalytic efficiency (Kcat/Km) compared to WT, in agreement with previous studies (27). These findings indicate that the S600T substitution in DENV RdRp enhances susceptibility to DMB220 not through increased binding but rather by decreasing binding and/or incorporation of the natural nucleotide substrate.

Molecular docking

The compound docked into the modified active site of the dengue polymerase structure 2J7U with a relatively high score and in interactions with the active site residues D533, D663 and D664 (Fig.5.). The compound is coordinated to both magnesium ions though interactions with its sulfoxide oxygens as well as through hydroxyl groups on the pyrimidine ring. The sulfoxide oxygens potentially have electrostatic interactions with the RNA template but minimal hydrophobic contacts. There are several other interactions with active site residues such as the main chain hydroxyl of A531 and the side chain of S710, with a possible induced dipole interaction with E733 on the phenyl portion. The docking thus supports the mechanism of action of this compound as a competitive inhibitor of Dengue NS5b polymerase. While the active site of Dengue polymerase is very much like that of HCV polymerase, the alignment of the active site of the recent

HCV ternary complex (54) with dengue structures 2J7U and 4V0R (59) reveals a different Mg coordination orientation from dengue; thus, this compound may have weak activity against HCV polymerase with altered interactions. Like integrase strand transfer inhibitors, this compound coordinates towards both Mg++ ions. Unlike integrase inhibitors with minimal hydrophobic contacts as observed in our simulations, this compound may not have broad class specificity or may bind to other polymerases differently. The lack of significant hydrophobic contacts may thus affect its potency. The addition of halogen groups on the phenyl ring may conceivably augment potency.

Inhibitory effects of DMB220 on HIV-1 integrase and reverse transcriptase

We also determined whether DMB220 can inhibit HIV-1integrase and reverse transcriptase, which also require metal ion cofactors at the active sites for catalysis. We observed that DMB 220 did not inhibit HIV-1 RT activity at concentrations as high as 100 μM. In the integrase strand transfer assay, DMB220 showed a weak inhibitory effect with an IC50 of 14 μM, in comparison with IC_{50s} of the approved HIV integrase inhibitors raltegravir, elvitegravir and dolutagravir, which ranged between 2.8 nM to 8.8 nM (Table 6). Thus, DMB220 possesses apparent specificity for the DENV NS5 polymerase.

Discussion

We have shown that a novel compound, DMB220, effectively inhibited the RdRp activity of NS5 polymerase of all four serotypes of DENV. Use of a cell-based assay has

validated this result, showing that DMB 220 possesses activity with EC_{50s} in the low micomolar range. DMB220 did not inhibit the reverse transcriptase activity of HIV-1 and exhibited only minimal inhibitory activity against HIV-1 integrase. These findings suggest that DMB220 is a selective anti DENV pan-serotype RdRp inhibitor.

DMB 220 is a pyridoxine-derived small-molecule inhibitorand represents a novel class of anti-RdRp agent. DMB220 was designed to chelate metal ion cofactors at the active site of RdRp. Our enzymatic and molecular modeling data prove that DMB220 competes with the natural NTP substrate for binding to the RdRp active site. Thus, this active-site non-nucleoside analogue inhibitor is different from classic NNIs that do not bind at the active site of the RdRp. Metal chelating inhibitors that target the active site of viral RdRp have been reported for hepatitis C virus. Derivatives of 4,5-dihydroxypyrimidine carboxylic acid and α,γ-diketo acid (DKA) (34, 35) have been developed to target HCV RdRp by chelating divalent metal ions at the active site of the polymerase. These anti-HCV inhibitors are competitive with nucleotides (55-57). Future work will assess whether DMB 220 possesses inhibitory effects against other polymerases from other viruses including that of HCV.

We have also demonstrated that the S600T substitution in RdRp can result in is hyper susceptibility to DMB220 by decreasing binding and/or incorporation of the natural nucleotide substrate rather than through increased binding of the inhibitor. This further supports the notion that DMB220 competes with natural nucleotide substrates for active-site binding. The serine residue at position 600 of DENV RdRp is located in the B motif

of the palm subdomain and is highly conserved among all viral RdRp enzymes. S600T was previously shown to be able to confer resistance to a nucleoside inhibitor of DENV RdRp, termed beta-d-2'-ethynyl-7-deaza-adenosine triphosphate (2'E-7D-ATP)(27). The counterpart S282T substitution in HCV RdRp NS5B was also shown to confer resistance to nucleoside analogue inhibitors (58-60). Our findings strongly suggest that DMB220 or its derivatives may also have the potential to mechanistically complement nucleoside analogue inhibitors in regard to inhibition of DENV replication. *Hyper-susceptibility is defined as an increase in susceptibility to a particular drug, i.e., lower concentrations of drug are needed to inhibit the replication of a mutated virus compared with wild-type. Currently, HIV represents the most extensively investigated agent in regard to antiviral drug-resistance and hyper-susceptibility and it is generally accepted that hyper-susceptibility can occur when the fold-change (FC) of EC_{50}/IC_{50} is <0.4. In the case of DENV antiviral research, no FDA-approved drug is yet available. Thus, it seems reasonable to state that the 3-fold change (FC=0.33) represents hyper-susceptibility.*

The prototype molecule DMB-220 exhibits cytotoxicity in the low micro molar range which is not unusual for antiviral compounds. However its low selectivity index, and the ratio of cytotoxicity to antiviral activity suggests that further development of this class of molecules is warranted. A more in depth study on the structure-activity relationship is being pursued and should result in better identification of the crucial chemical moieties. Our aim is to improve the SI to above 1000 before undertaking preclinical studies.

Antimicrobial Agents and Chemotherapy

In summary, we have shown that the pyridoxine-derived active site inhibitor DMB-220 can inhibit DENV RdRp activity and viral replication in tissue culture. The compound apparently acts as a competitive inhibitor of natural nucleotide substrates for binding to the active site of the enzyme. Our study demonstrates that chelation of active site metals within the viral polymerase may be a valid strategy for the development of novel and efficacious anti-DENV compounds.This is also the first report of an active-site non-nucleoside inhibitor of DENV RdRp against which an NI-resistant substitution can confer hyper-susceptibility.

FIGURE LEGENDS

Fig.1. Structure and reaction scheme of the chemical synthesis of compound DMB220. Reagents and conditions: a) MS-Cl, DCM TEA R.T; b) $ArSO_2$-Na, DMF; c) MCPBA 70%, DCM; d) TFAA $CHCl_3$; e) MnO_2 $CHCl_3$; f) TMSOK, I_2, MeOH; g) 70% HCOOH aq; h) H_2NOH aq, Py.

Fig.2. Purification and activity of recombinant NS5 polymerase domains of the four serotypes of DENV. (A) Coomassie brilliant blue staining of purified NS5 polymerase domains after 10% SDS-PAGE. MW, molecular size standards, in kilo daltons. The positions of purified recombinant NS5 polymerase domains are indicated on the right. (B) Activity of recombinant DENV NS5 polymerase domains as assessed using a(-) 3'UTR RNA template by filter-binding RdRp assay as described in Materials and Methods.

Values are means of two independent experiments. Error bars represent standard deviations.

Fig. 3. Dose-response curves showing inhibition by DMB220 of the activity of DENV1-4 polymerase and the S600T mutant. Inhibitory effect was determined by in vitro filter binding RdRp assay using purified enzymes and DENV (-) 3'UTR RNA template in assay buffer containing 40 mM Tris-HCL, pH 7.0, 10 mM NaCL, 1 mM $MgCL_2$, 0.5 mM $MnCL_2$, 0.001% Triton X-100, 10 µM cysteine and 4 µM NTPs including ^3H -CTP as tracer. The data shown are from one representative experiment. The IC50 values were determined from the results of three independent experiments and are summarized in Table 2.

Fig. 4. The inhibition constants (Ki) of DMB220 for WT (A) and S600T (B) enzymes were determined by graphical methods and use of a Dixon plot. The plots demonstrate the inhibitory effect of DMB220 in the presence of varying NTPs added at concentrations of 1.3 µM, 4 µM and 8 µM, respectively. The Ki values of DMB220 for the WT and S600T enzymes are 3.2± 0.7 µM and 2.9 ± 0.6 µM respectively. The graphical representations resulted from one representative experiment performed in duplicate and data are presented as means ± SD. The reported Ki was calculated from the results of three independent experiments and is expressed as mean ± SD in Table 5.

Fig. 5. Docking of the compound into the active site of the Dengue polymerase structure (PDB ID:2J7U) (24) (Blue cartoon structure). The compound docks in close proximity to

and interacting with active site residues D663 and S661. The active site is shown as surface coloured by standard CPK coloration. Blue represents surface-exposed nitrogen groups and red represents surface-exposed oxygen groups. The possible location of a putative second active site Mg++ ion was superimposed into the 2J7U structure of the HIV RT structure 1RTD by multiple sequential partial sequence and structure overlay. Prior to compound docking, a short single RNA strand (5'UUUAGUU) was retrieved from the PDB structure 1WMQ and docked into the prepared 2J7U structure using Autodock Tools and Autodock Vina. Structure visualization was by PyMol.

References:

1. **Westaway, E. G., M. A. Brinton, S. Gaidamovich, M. C. Horzinek, A. Igarashi, L. Kaariainen, D. K. Lvov, J. S. Porterfield, P. K. Russell, and D. W. Trent. 1985. Flaviviridae. Intervirology 24:183-192.**
2. **Guzman, M. G., S. B. Halstead, H. Artsob, P. Buchy, J. Farrar, D. J. Gubler, E. Hunsperger, A. Kroeger, H. S. Margolis, E. Martinez, M. B. Nathan, J. L. Pelegrino, C. Simmons, S. Yoksan, and R. W. Peeling. 2010. Dengue: a continuing global threat. Nat Rev Microbiol 8:S7-16.**
3. **Guzman, M. G., and E. Harris. 2015. Dengue. Lancet 385:453-465.**
4. **Murray, N. E., M. B. Quam, and A. Wilder-Smith. 2013. Epidemiology of dengue: past, present and future prospects. Clin Epidemiol 5:299-309.**
5. **Halstead, S. B., and S. N. Cohen. 2015. Dengue Hemorrhagic Fever at 60 Years: Early Evolution of Concepts of Causation and Treatment. Microbiol Mol Biol Rev 79:281-291.**
6. **Costa, R. L., C. M. Voloch, and C. G. Schrago. 2012. Comparative evolutionary epidemiology of dengue virus serotypes. Infect Genet Evol 12:309-314.**
7. **Wilson, M. E., and L. H. Chen. 2015. Dengue: update on epidemiology. Curr Infect Dis Rep 17:457.**
8. **Bhatt, S., P. W. Gething, O. J. Brady, J. P. Messina, A. W. Farlow, C. L. Moyes, J. M. Drake, J. S. Brownstein, A. G. Hoen, O. Sankoh, M. F. Myers, D. B. George, T. Jaenisch, G. R. Wint, C. P. Simmons, T. W. Scott, J. J. Farrar, and S. I. Hay. 2013. The global distribution and burden of dengue. Nature 496:504-507.**
9. **Woodland, D. L. 2015. Vaccines against dengue virus. Viral Immunol 28:75.**
10. **Tsai, W. Y., A. Durbin, J. J. Tsai, S. C. Hsieh, S. Whitehead, and W. K. Wang. 2015. Complexity of neutralization antibodies against multiple dengue**

viral serotypes after heterotypic immunization and secondary infection revealed by in-depth analysis of cross-reactive antibodies. J Virol.

11. Ramakrishnan, L., M. R. Pillai, and R. R. Nair. 2015. Dengue vaccine development: strategies and challenges. Viral Immunol 28:76-84.
12. Xie, X., J. Zou, Q. Y. Wang, and P. Y. Shi. 2015. Targeting dengue virus NS4B protein for drug discovery. Antiviral Res 118:39-45.
13. Wu, H., S. Bock, M. Snitko, T. Berger, T. Weidner, S. Holloway, M. Kanitz, W. E. Diederich, H. Steuber, C. Walter, D. Hofmann, B. Weissbrich, R. Spannaus, E. G. Acosta, R. Bartenschlager, B. Engels, T. Schirmeister, and J. Bodem. 2015. Novel dengue virus NS2B/NS3 protease inhibitors. Antimicrob Agents Chemother 59:1100-1109.
14. Luo, D., S. G. Vasudevan, and J. Lescar. 2015. The flavivirus NS2B-NS3 protease-helicase as a target for antiviral drug development. Antiviral Res 118:148-158.
15. Lim, S. P., C. G. Noble, and P. Y. Shi. 2015. The dengue virus NS5 protein as a target for drug discovery. Antiviral Res 119:57-67.
16. Lim, S. P., Q. Y. Wang, C. G. Noble, Y. L. Chen, H. Dong, B. Zou, F. Yokokawa, S. Nilar, P. Smith, D. Beer, J. Lescar, and P. Y. Shi. 2013. Ten years of dengue drug discovery: progress and prospects. Antiviral Res 100:500-519.
17. Noble, C. G., Y. L. Chen, H. Dong, F. Gu, S. P. Lim, W. Schul, Q. Y. Wang, and P. Y. Shi. 2010. Strategies for development of Dengue virus inhibitors. Antiviral Res 85:450-462.
18. Bollati, M., K. Alvarez, R. Assenberg, C. Baronti, B. Canard, S. Cook, B. Coutard, E. Decroly, X. de Lamballerie, E. A. Gould, G. Grard, J. M. Grimes, R. Hilgenfeld, A. M. Jansson, H. Malet, E. J. Mancini, E. Mastrangelo, A. Mattevi, M. Milani, G. Moureau, J. Neyts, R. J. Owens, J. Ren, B. Selisko, S. Speroni, H. Steuber, D. I. Stuart, T. Unge, and M. Bolognesi. 2010. Structure and functionality in flavivirus NS-proteins: perspectives for drug design. Antiviral Res 87:125-148.
19. Malet, H., N. Masse, B. Selisko, J. L. Romette, K. Alvarez, J. C. Guillemot, H. Tolou, T. L. Yap, S. Vasudevan, J. Lescar, and B. Canard. 2008. The flavivirus polymerase as a target for drug discovery. Antiviral Res 80:23-35.
20. Tomlinson, S. M., R. D. Malmstrom, A. Russo, N. Mueller, Y. P. Pang, and S. J. Watowich. 2009. Structure-based discovery of dengue virus protease inhibitors. Antiviral Res 82:110-114.
21. Beesetti, H., N. Khanna, and S. Swaminathan. 2014. Drugs for dengue: a patent review (2010-2014). Expert Opin Ther Pat 24:1171-1184.
22. Zhao, Y., T. S. Soh, J. Zheng, K. W. Chan, W. W. Phoo, C. C. Lee, M. Y. Tay, K. Swaminathan, T. C. Cornvik, S. P. Lim, P. Y. Shi, J. Lescar, S. G. Vasudevan, and D. Luo. 2015. A crystal structure of the Dengue virus NS5 protein reveals a novel inter-domain interface essential for protein flexibility and virus replication. PLoS Pathog 11:e1004682.
23. Lim, S. P., J. H. Koh, C. C. Seh, C. W. Liew, A. D. Davidson, L. S. Chua, R. Chandrasekaran, T. C. Cornvik, P. Y. Shi, and J. Lescar. 2013. A crystal structure of the dengue virus non-structural protein 5 (NS5) polymerase

delineates interdomain amino acid residues that enhance its thermostability and de novo initiation activities. J Biol Chem 288:31105-31114.

24. Yap, T. L., T. Xu, Y. L. Chen, H. Malet, M. P. Egloff, B. Canard, S. G. Vasudevan, and J. Lescar. 2007. Crystal structure of the dengue virus RNA-dependent RNA polymerase catalytic domain at 1.85-angstrom resolution. J Virol 81:4753-4765.

25. Steitz, T. A., and J. A. Steitz. 1993. A general two-metal-ion mechanism for catalytic RNA. Proc Natl Acad Sci U S A 90:6498-6502.

26. Ackermann, M., and R. Padmanabhan. 2001. De novo synthesis of RNA by the dengue virus RNA-dependent RNA polymerase exhibits temperature dependence at the initiation but not elongation phase. J Biol Chem 276:39926-39937.

27. Latour, D. R., A. Jekle, H. Javanbakht, R. Henningsen, P. Gee, I. Lee, P. Tran, S. Ren, A. K. Kutach, S. F. Harris, S. M. Wang, S. J. Lok, D. Shaw, J. Li, G. Heilek, K. Klumpp, D. C. Swinney, and J. Deval. 2010. Biochemical characterization of the inhibition of the dengue virus RNA polymerase by beta-d-2'-ethynyl-7-deaza-adenosine triphosphate. Antiviral Res 87:213-222.

28. Yin, Z., Y. L. Chen, W. Schul, Q. Y. Wang, F. Gu, J. Duraiswamy, R. R. Kondreddi, P. Niyomrattanakit, S. B. Lakshminarayana, A. Goh, H. Y. Xu, W. Liu, B. Liu, J. Y. Lim, C. Y. Ng, M. Qing, C. C. Lim, A. Yip, G. Wang, W. L. Chan, H. P. Tan, K. Lin, B. Zhang, G. Zou, K. A. Bernard, C. Garrett, K. Beltz, M. Dong, M. Weaver, H. He, A. Pichota, V. Dartois, T. H. Keller, and P. Y. Shi. 2009. An adenosine nucleoside inhibitor of dengue virus. Proc Natl Acad Sci U S A 106:20435-20439.

29. Hocharoen, L., and J. A. Cowan. 2009. Metallotherapeutics: novel strategies in drug design. Chemistry 15:8670-8676.

30. Carcelli, M., D. Rogolino, A. Bacchi, G. Rispoli, E. Fisicaro, C. Compari, M. Sechi, A. Stevaert, and L. Naesens. 2014. Metal-chelating 2-hydroxyphenyl amide pharmacophore for inhibition of influenza virus endonuclease. Mol Pharm 11:304-316.

31. Carcelli, M., D. Rogolino, M. Sechi, G. Rispoli, E. Fisicaro, C. Compari, N. Grandi, A. Corona, E. Tramontano, C. Pannecouque, and L. Naesens. 2014. Antiretroviral activity of metal-chelating HIV-1 integrase inhibitors. Eur J Med Chem 83:594-600.

32. Rogolino, D., M. Carcelli, A. Bacchi, C. Compari, L. Contardi, E. Fisicaro, A. Gatti, M. Sechi, A. Stevaert, and L. Naesens. 2015. A versatile salicyl hydrazonic ligand and its metal complexes as antiviral agents. J Inorg Biochem 150:9-17.

33. DuBois, R. M., P. J. Slavish, B. M. Baughman, M. K. Yun, J. Bao, R. J. Webby, T. R. Webb, and S. W. White. 2012. Structural and biochemical basis for development of influenza virus inhibitors targeting the PA endonuclease. PLoS Pathog 8:e1002830.

34. Koch, U., B. Attenni, S. Malancona, S. Colarusso, I. Conte, M. Di Filippo, S. Harper, B. Pacini, C. Giomini, S. Thomas, I. Incitti, L. Tomei, R. De Francesco, S. Altamura, V. G. Matassa, and F. Narjes. 2006. 2-(2-Thienyl)-5,6-dihydroxy-4-carboxypyrimidines as inhibitors of the hepatitis C virus

NS5B polymerase: discovery, SAR, modeling, and mutagenesis. J Med Chem 49:1693-1705.

35. Summa, V., A. Petrocchi, P. Pace, V. G. Matassa, R. De Francesco, S. Altamura, L. Tomei, U. Koch, and P. Neuner. 2004. Discovery of alpha,gamma-diketo acids as potent selective and reversible inhibitors of hepatitis C virus NS5b RNA-dependent RNA polymerase. J Med Chem 47:14-17.

36. Stranix, B., F. Beaulieu, J.-E. Bouchard, G. Milot, Z. Wang, and R. Ruel. 2009. HIV integrase inhibitors from pyridoxine. US patent US8742123 B2.

37. Usme-Ciro, J. A., J. A. Lopera, L. Enjuanes, F. Almazan, and J. C. Gallego-Gomez. 2014. Development of a novel DNA-launched dengue virus type 2 infectious clone assembled in a bacterial artificial chromosome. Virus Res 180:12-22.

38. Gong, E. Y., H. Kenens, T. Ivens, K. Dockx, K. Vermeiren, G. Vandercruyssen, B. Devogelaere, P. Lory, and G. Kraus. 2013. Expression and purification of dengue virus NS5 polymerase and development of a high-throughput enzymatic assay for screening inhibitors of dengue polymerase. Methods Mol Biol 1030:237-247.

39. Selisko, B., H. Dutartre, J. C. Guillemot, C. Debarnot, D. Benarroch, A. Khromykh, P. Despres, M. P. Egloff, and B. Canard. 2006. Comparative mechanistic studies of de novo RNA synthesis by flavivirus RNA-dependent RNA polymerases. Virology 351:145-158.

40. Medina, F., J. F. Medina, C. Colon, E. Vergne, G. A. Santiago, and J. L. Munoz-Jordan. 2012. Dengue virus: isolation, propagation, quantification, and storage. Curr Protoc Microbiol Chapter 15:Unit 15D 12.

41. Gong, E. Y., M. Clynhens, T. Ivens, P. Lory, K. Simmen, and G. Kraus. 2013. Cell-based antiviral assays for screening and profiling inhibitors against dengue virus. Methods Mol Biol 1030:185-194.

42. Farias, K. J., P. R. Machado, and B. A. da Fonseca. 2013. Chloroquine inhibits dengue virus type 2 replication in Vero cells but not in C6/36 cells. ScientificWorldJournal 2013:282734.

43. Xu, H. T., J. L. Martinez-Cajas, M. L. Ntemgwa, D. Coutsinos, F. A. Frankel, B. G. Brenner, and M. A. Wainberg. 2009. Effects of the K65R and K65R/M184V reverse transcriptase mutations in subtype C HIV on enzyme function and drug resistance. Retrovirology 6:14.

44. Xu, H. T., E. L. Asahchop, M. Oliveira, P. K. Quashie, Y. Quan, B. G. Brenner, and M. A. Wainberg. 2011. Compensation by the E138K mutation in HIV-1 reverse transcriptase for deficits in viral replication capacity and enzyme processivity associated with the M184I/V mutations. J Virol 85:11300-11308.

45. Xu, H. T., S. P. Colby-Germinario, P. K. Quashie, R. Bethell, and M. A. Wainberg. 2015. Subtype-specific analysis of the K65R substitution in HIV-1 that confers hypersusceptibility to a novel nucleotide-competing reverse transcriptase inhibitor. Antimicrob Agents Chemother 59:3189-3196.

46. Quashie, P. K., T. Mesplede, Y. S. Han, M. Oliveira, D. N. Singhroy, T. Fujiwara, M. R. Underwood, and M. A. Wainberg. 2012. Characterization of

the R263K mutation in HIV-1 integrase that confers low-level resistance to the second-generation integrase strand transfer inhibitor dolutegravir. J Virol 86:2696-2705.

47. Bar-Magen, T., D. A. Donahue, E. I. McDonough, B. D. Kuhl, V. H. Faltenbacher, H. Xu, V. Michaud, R. D. Sloan, and M. A. Wainberg. 2010. HIV-1 subtype B and C integrase enzymes exhibit differential patterns of resistance to integrase inhibitors in biochemical assays. AIDS 24:2171-2179.

48. Selisko, B., S. Potisopon, R. Agred, S. Priet, I. Varlet, Y. Thillier, C. Sallamand, F. Debart, J. J. Vasseur, and B. Canard. 2012. Molecular basis for nucleotide conservation at the ends of the dengue virus genome. PLoS Pathog 8:e1002912.

49. Notredame, C., D. G. Higgins, and J. Heringa. 2000. T-Coffee: A novel method for fast and accurate multiple sequence alignment. J Mol Biol 302:205-217.

50. Kumarevel, T., H. Mizuno, and P. K. Kumar. 2005. Structural basis of HutP-mediated anti-termination and roles of the Mg2+ ion and L-histidine ligand. Nature 434:183-191.

51. Niyomrattanakit, P., K. F. Wan, K. Y. Chung, S. N. Abas, C. C. Seh, H. Dong, C. C. Lim, A. T. Chao, C. B. Lee, S. Nilar, J. Lescar, P. Y. Shi, D. Beer, and S. P. Lim. 2015. Stabilization of dengue virus polymerase in de novo initiation assay provides advantages for compound screening. Antiviral Res 119:36-46.

52. Takhampunya, R., S. Ubol, H. S. Houng, C. E. Cameron, and R. Padmanabhan. 2006. Inhibition of dengue virus replication by mycophenolic acid and ribavirin. J Gen Virol 87:1947-1952.

53. Yang, C. C., H. S. Hu, R. H. Wu, S. H. Wu, S. J. Lee, W. T. Jiaang, J. H. Chern, Z. S. Huang, H. N. Wu, C. M. Chang, and A. Yueh. 2014. A novel dengue virus inhibitor, BP13944, discovered by high-throughput screening with dengue virus replicon cells selects for resistance in the viral NS2B/NS3 protease. Antimicrob Agents Chemother 58:110-119.

54. Appleby, T. C., J. K. Perry, E. Murakami, O. Barauskas, J. Feng, A. Cho, D. Fox, 3rd, D. R. Wetmore, M. E. McGrath, A. S. Ray, M. J. Sofia, S. Swaminathan, and T. E. Edwards. 2015. Viral replication. Structural basis for RNA replication by the hepatitis C virus polymerase. Science 347:771-775.

55. Powdrill, M. H., J. A. Bernatchez, and M. Gotte. 2010. Inhibitors of the Hepatitis C Virus RNA-Dependent RNA Polymerase NS5B. Viruses 2:2169-2195.

56. Powdrill, M. H., J. Deval, F. Narjes, R. De Francesco, and M. Gotte. 2010. Mechanism of hepatitis C virus RNA polymerase inhibition with dihydroxypyrimidines. Antimicrob Agents Chemother 54:977-983.

57. Deore, R. R., G. S. Chen, C. S. Chen, P. T. Chang, M. H. Chuang, T. R. Chern, H. C. Wang, and J. W. Chern. 2012. 2-hydroxy-1-oxo-1,2-dihydroisoquinoline-3-carboxylic acid with inbuilt beta-N-hydroxy-gamma-keto-acid pharmacophore as HCV NS5B polymerase inhibitors. Curr Med Chem 19:613-624.

772 **58. Tong, X., L. Li, K. Haines, and I. Najera. 2014. Identification of the NS5B**
773 **S282T resistant variant and two novel amino acid substitutions that affect**
774 **replication capacity in hepatitis C virus-infected patients treated with**
775 **mericitabine and danoprevir. Antimicrob Agents Chemother 58:3105-3114.**
776 **59. Migliaccio, G., J. E. Tomassini, S. S. Carroll, L. Tomei, S. Altamura, B. Bhat,**
777 **L. Bartholomew, M. R. Bosserman, A. Ceccacci, L. F. Colwell, R. Cortese, R.**
778 **De Francesco, A. B. Eldrup, K. L. Getty, X. S. Hou, R. L. LaFemina, S. W.**
779 **Ludmerer, M. MacCoss, D. R. McMasters, M. W. Stahlhut, D. B. Olsen, D. J.**
780 **Hazuda, and O. A. Flores. 2003. Characterization of resistance to non-**
781 **obligate chain-terminating ribonucleoside analogs that inhibit hepatitis C**
782 **virus replication in vitro. J Biol Chem 278:49164-49170.**
783 **60. Dutartre, H., C. Bussetta, J. Boretto, and B. Canard. 2006. General catalytic**
784 **deficiency of hepatitis C virus RNA polymerase with an S282T mutation and**
785 **mutually exclusive resistance towards 2'-modified nucleotide analogues.**
786 **Antimicrob Agents Chemother 50:4161-4169.**
787
788

789

790
791
792 **TABLE 1.** Steady-state kinetic parameters of NTPs for all four serotypes of DENV NS5

793 polymerase

	DENV1	DENV2	DENV3	DENV4
K_m (μM)	3.5 ± 0.8	4.0± 1.0	3.7 ± 0.9	3.3 ± 0.7
K_{cat} (min^{-1})	0.046 ± 0.001	0.088 ± 0.004	0.052 ± 0.002	0.142 ± 0.005
K_{cat}/K_m (min^{-1} μM^{-1})	0.013	0.022	0.014	0.043
FC [a]	0.3	0.51	0.33	1

794

795 [a] FC: fold-change in catalytic efficiency (K_{cat}/K_m) relative to DENV4 NS5 polymerase.

796 Data represent means ± standard deviation (SD) of at least 2 independent experiments.

797

798 **TABLE 2.** Inhibition of RdRp activity of all four serotypes of dengue virus NS5

799 polymerase[a]

	IC50 (μM)				
Compounds	DENV1	DENV2	DENV3	DENV4	S600T[b]
DMB220	5.7±0.9	6.0±0.4	6.7±1.0	5.0±0.9	1. 8± 0.2
3'-dGTP	0.6±0.1	0.4±0.2	0.6±0.3	0.5±0.1	0.5 ± 0.2

800 [a] IC_{50} (50% drug inhibitory concentration) values were determined by in vitro filter
801 binding RdRp assay using purified DENV NS5 polymerase domains and DENV (-
802)3'UTR RNA template at 4 μM NTPs including ^{3}H -CTP as tracer. Data represent the
803 means ± standard deviation (SD) of 3 independent experiments.
804 [b] The S600T substitution was introduced into the DENV2 NS5 polymerase domain by
805 site-directed mutagenesis.

806

807 **TABLE3.** Tissue culture antiviral activity against the four serotypes of dengue virus

	EC50 (μM) [a]				CC50(μM) [b]
	DENV1	DENV2	DENV3	DENV4	
DMB220	2.7 ± 0.4	2.8 ± 0.6	2.7 ± 0.6	2.2 ± 0.5	18 ± 3.2
MPA [c]	0.5 ± 0.1	0.6± 0.1	0.4 ± 0.2	0.5 ± 0.2	>50

808

809 [a]The 50% effective concentration (EC_{50}) was determined in BHK-21 cells using the
810 Promega Viral ToxGlo Assay. Data represent the means ± standard deviation (SD) of 2-3
811 independent experiments.

[b]The 50% cytotoxic concentration (CC_{50}) was determined in BHK-21 cells using the Promega Viral ToxGlo Assay

[c]MPA: mycophenolic acid.

TABLE 4. Influence of NTP concentrations on the inhibitory activity of DMB220 on DENV serotype 2 polymerase activity [a]

NTPs (μM)	DMB220 IC_{50} (μM)
1.3	4.1 ± 0.3
4	5.7 ± 0.8
12	15.1 ± 2.8
36	32.2 ± 3.5

[a] The effect of NTP concentration on the inhibitory potency of DMB220 was evaluated by filter-binding RdRp assay in the presence of various concentrations of NTPs and DMB220. Data represent means ± standard deviation (SD) of 3 independent experiments.

TABLE 5. Kinetic parameters for WT DENV2 NS5 RdRp and S600T mutated RdRp

	WT	S600T	Fold-change (S600T/WT)
K_m (μM)	3.8 ± 0.7	11.5 ± 1.3	3.0
K_{cat} (min^{-1})	0.082 ± 0.006	0.033 ± 0.003	0.4
K_{cat}/K_m (min^{-1} μM^{-1})	0.022	0.003	0.14

K_i (μM)	3.2 ± 0.7	2.9 ± 0.6	0.9
K_i/K_m	0.84	0.25	0.3

TABLE 6. Inhibition of HIV-1 integrase activity as assessed in a cell-free strand transfer assay [a]

Compound	IC50 (nM)
DMB220	14260 ± 3480
Dolutegravir	8.1 ± 0.2
Elvitegravir	2.8 ± 1.4
Raltegravir	8.8 ± 1.4

[a] IC_{50} (50% drug inhibitory concentration) values were determined in standard strand transfer assays using purified recombinant HIV-1 integrase. Data represent means ± standard deviation of 2 independent experiments.

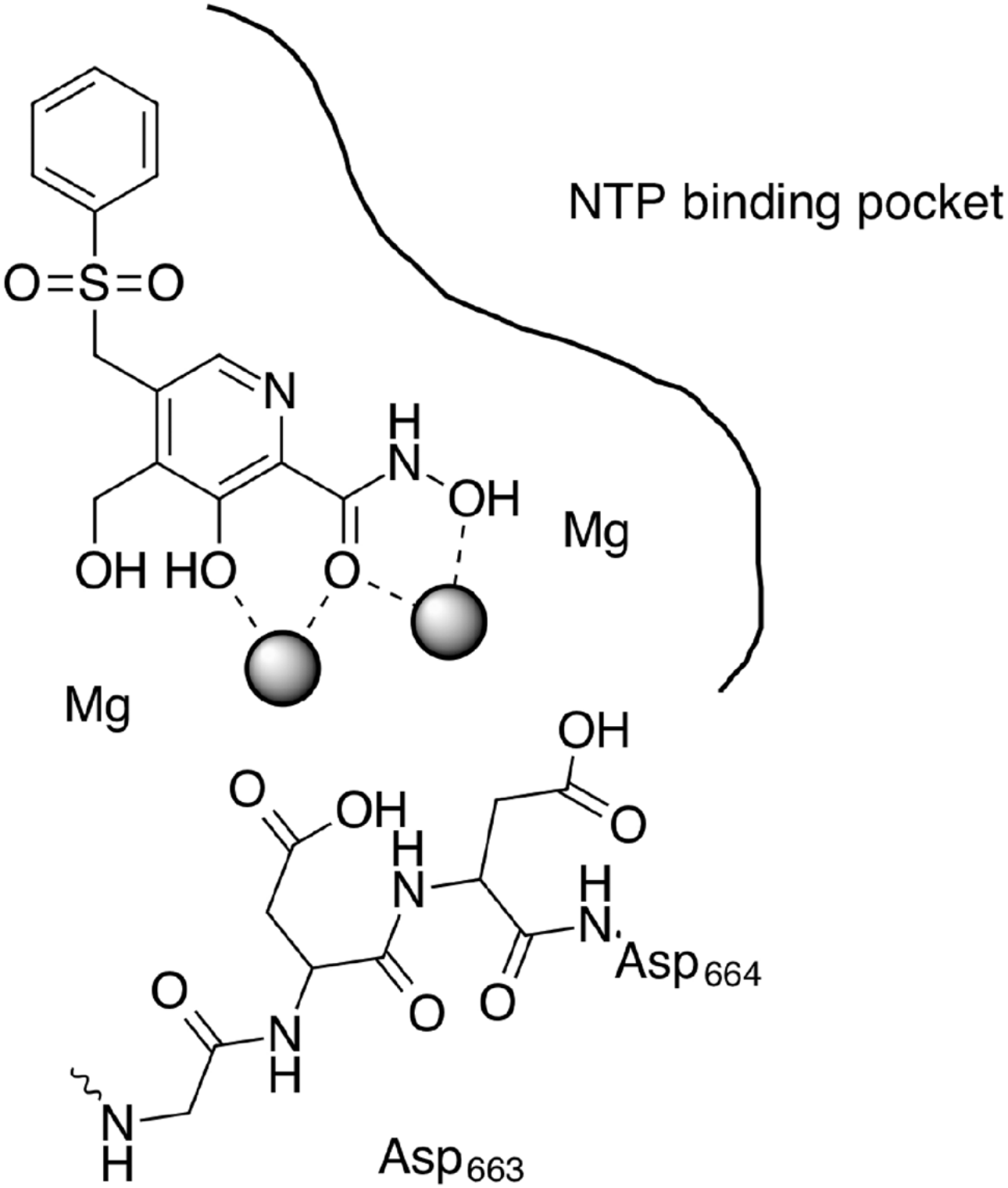

A

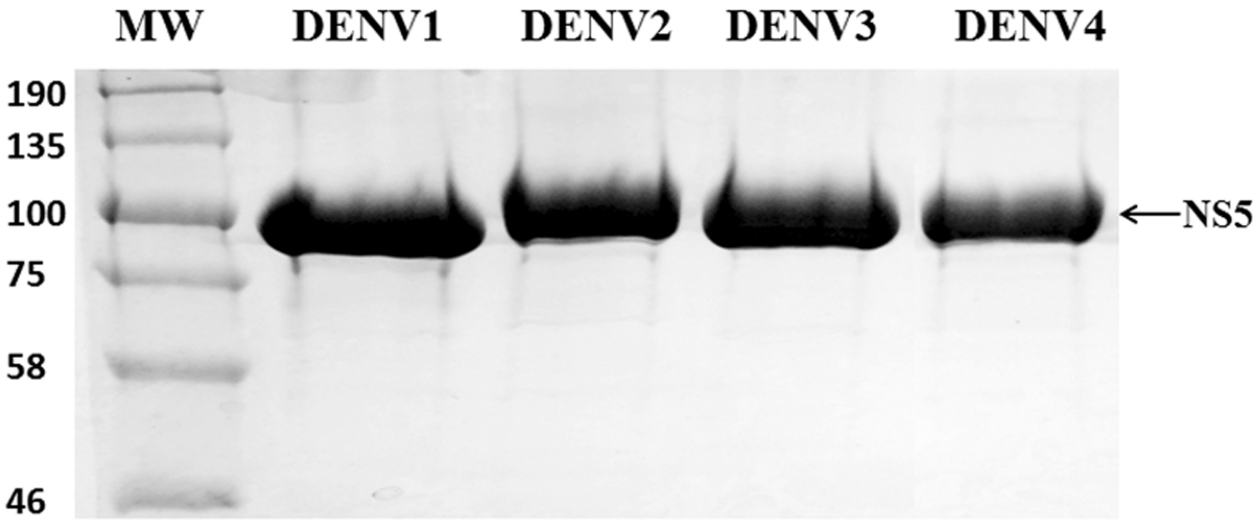

B